

Experimental study of slider dynamics induced by contacts with disk asperities

Wenping Song · Liane Matthes · Andrey Ovcharenko ·
Bernhard Knigge · Frank E. Talke

Received: 31 October 2012 / Accepted: 21 May 2013 / Published online: 6 June 2013
© Springer-Verlag Berlin Heidelberg 2013

Abstract Vertical vibrations at the slider leading edge excited by a disk asperity were investigated in a drive level system, using laser Doppler vibrometry and acoustic emission (AE) sensors. The flying height change at the leading edge of a thermal flying-height control slider was measured for different power inputs to the heater element. The maximum spacing change at the slider leading edge was found to be about 4 nm for an asperity of 26 nm height and 1.1 μm width. A method was investigated to produce “artificial asperities” on a disk surface using a nano-indenter. The geometry of the “artificial asperities” was characterized using an atomic force microscope. In addition, a spin stand was used to analyze the AE signal of slider vibrations induced by contacts with the “artificial asperities”. First and second pitch modes of the slider were observed.

1 Introduction

The spacing between slider and disk has decreased to a few nanometers (Kurita et al. 2006; Nikitin et al. 2007; Zheng et al. 2009). As a consequence, the flying characteristics of a slider are strongly influenced by slider-disk contacts, especially caused by asperities on the disk. Flying height

changes of the slider can cause errors during read or write process. In addition, slider-disk contacts can result in data loss of information recorded on a disk surface (Ovcharenko et al. 2010).

Slider dynamics induced by slider-disk contacts have been investigated by many researchers. Tanaka et al. (2001) investigated the dynamics of a nano-slider using LDV, friction sensors and AE sensors during slider-disk contacts. Li et al. (2009) investigated the flying characteristics of a TFC slider using AE sensors and friction sensors. They showed that a TFC slider can fly stably with a flying height of 1 nm without physical contacts with the disk. The effect of disk lubricant on the slider dynamics was investigated by Deoras and Talke (2003) who found that slider vibrations increase with increasing the thickness of the lubricant. The vertical, down-track and off-track slider vibrations induced by slider contact with a lubricant were studied by (Vangipuram and Bogy 2010).

In addition, a number of investigations have studied slider dynamics induced by disk asperities. Knigge and Talke (2001) investigated slider dynamics when a slider flies over artificial disk defects such as scratches and bumps. In their study, the height of the pileup of the scratches was around 100 nm and the height of the bumps was about 130 nm. They also found that slider vibrations increase with increasing lubricant thickness, in agreement with work done by Deoras and Talke (2003). Su et al. (2011) studied slider dynamics when a slider flies over a bump with a height of 9 nm. Vibrations of about 300 kHz were observed for three different air bearing surface (ABS) designs. Additional methods of preparing artificial asperities were proposed by Wallash et al. (2008). They presented artificial asperities produced by scratch and indentation tests using different tips and loads to control the shape of the artificial asperities. Wallash et al. (2008)

W. Song (✉)
Harbin Institute of Technology, Harbin, China
e-mail: wenping.song1985@gmail.com

W. Song · L. Matthes · F. E. Talke
Center for Magnetic Recording Research, University
of California, San Diego, CA, USA

A. Ovcharenko · B. Knigge
Western Digital Corporation, San Jose, CA, USA

also studied resistance changes of the read element induced by contacts between a slider and disk defects.

Although the above studies have addressed contacts between slider and disk in spin stand tests, slider dynamics induced by contacts with disk asperities in a real hard disk drive have not been investigated extensively. This study is intended to fill this gap by investigating the slider dynamics induced by contacts with disk asperities in a commercial drive. The effect of power input to the heater element is investigated. In addition, “artificial asperities” were produced using a nano-indentor, and slider vibrations induced by contacts with the “artificial asperities” are studied in a spin stand.

2 Slider dynamics induced by a disk asperity in a hard disk drive

2.1 Experimental setup

Figure 1 shows the schematic of a drive level setup to measure slider dynamics induced by contacts with disk asperities. As shown in Fig. 1, the laser beam of an LDV (Polytec OFV-512) is focused on the gimbal close to the leading edge of the slider through a cutout in the top cover of the hard disk drive. The disk rotates at rotational velocity of 7,200 rpm. An AE sensor (Mistras S9208), which is rigidly mounted on the E-block, is used to detect contacts between the slider and asperities on the top surface of the disk. A commercially available amplifier (Mistras 2/4/6C) is used to amplify the AE signal by a factor of

1,000. In order to compare the LDV and AE measurements, the LDV and AE signals are captured synchronously at a frequency of 2 MHz using a magnetic servo index on the disk.

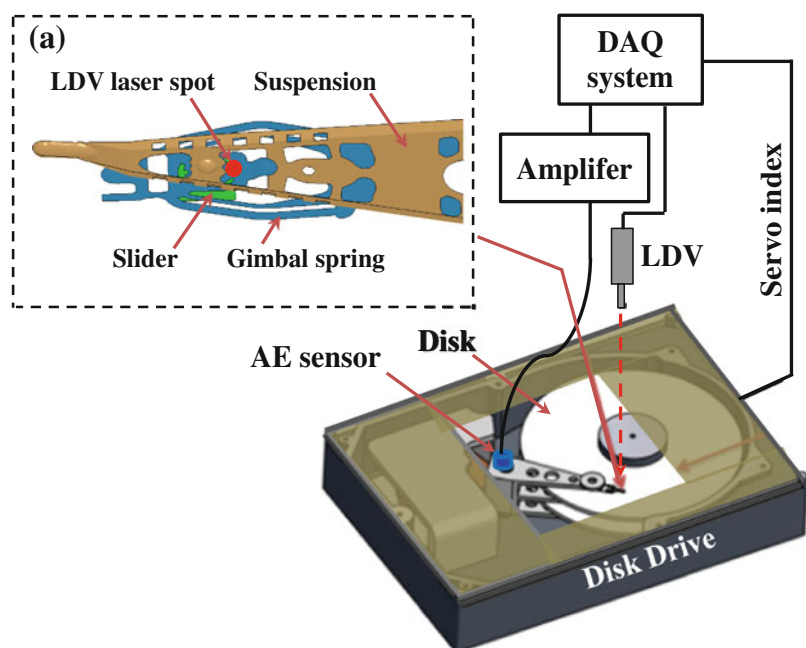
2.2 Results and discussion

In this investigation, disk defects are first mapped based on the read-back signal. Then, the slider dynamics induced by disk asperities is measured using the experimental setup shown in Fig. 1. During the measurements, the slider flies over a track with a mapped defect. After the test, the shape of the disk defect is characterized using an AFM.

Figure 2 shows the AFM measurements of the defect tested in this study. The profile of the defect in Fig. 2a at the dashed line is shown in Fig. 2b. We observe that the height of the asperity is 26 nm and the width is 1.1 μm . Figure 2c shows the three dimensional image of the disk asperity. It is apparent that contacts between the slider and the defect occur if the slider flies over this defect, since the physical spacing between the thermal protrusion of the TFC slider and the disk surface is only a few nanometers. i.e., much less than the height of the defect.

Figure 3a shows LDV measurements for the vertical velocity at the slider leading edge as a function of time for $P_{\text{heat}} = 100 \text{ mW}$. The result shown in Fig. 3a is the averaged velocity for 200 measurements using the servo index as a trigger for data acquisition. The fast Fourier transform (FFT) of the LDV signal of Fig. 3a is shown in Fig. 3b. The low frequencies at 120 Hz and the higher order harmonics at 240, 360, and 480 Hz in Fig. 3b are related to the

Fig. 1 Schematic of experimental setup for measuring slider dynamics induced by contacts with disk asperity



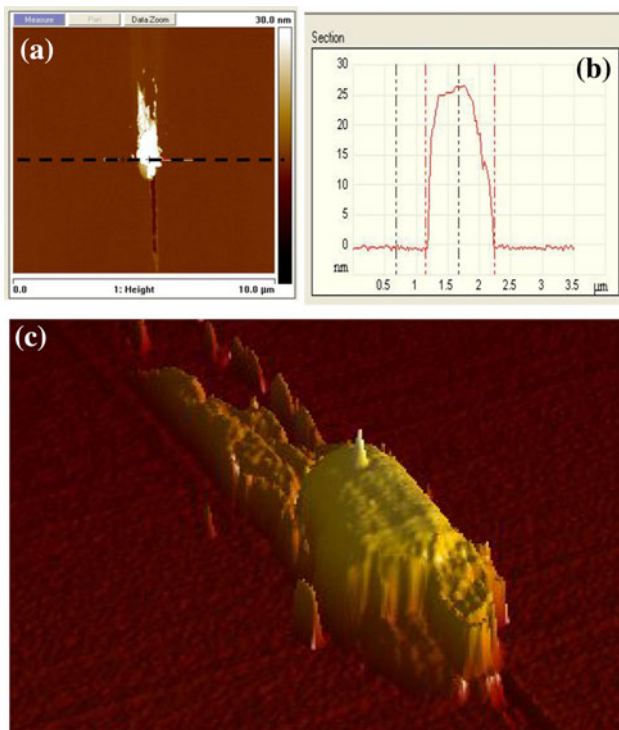


Fig. 2 AFM measurements of defect on disk surface

disk angular velocity of 7,200 rpm. In addition, we observe two other distinct frequencies at 126 and 261 kHz. The frequency at 126 kHz corresponds to the first ABS pitch mode and the frequency at 261 kHz corresponds to the second ABS pitch mode. Figure 3c shows the slider vertical velocity excluding the effect of the 120 Hz frequency after band-passing the signal at frequencies of 20–800 kHz.

Figure 4a shows the flying height change at the leading edge of the slider as a function of time, calculated by integrating the LDV velocity signal shown in Fig. 3c. The AE signal is shown in Fig. 4b for comparison. From Fig. 4a and b, we observe that vibrations observed by the LDV and the AE sensors are in good agreement. The maximum amplitude of flying height change ΔFH_{\max} is 1 nm in this case.

Figure 5 shows the maximum amplitude of slider displacements as a function of the power input to the heater element P_{heat} . The results for the slider flying on the track with the defect and for flying on the reference track without defects are shown as solid and dashed lines, respectively. The reference track is chosen to be 100 tracks away from the track with the defect. As can be seen from Fig. 5, when the slider flies on the reference track, the maximum amplitude of slider vibrations is about 0.5 nm for $P_{\text{heat}} \leq 165$ mW. This indicates that contacts between the slider and the defect are absent. A sharp increase is observed at $P_{\text{heat}} = 172$ mW, corresponding to the touch

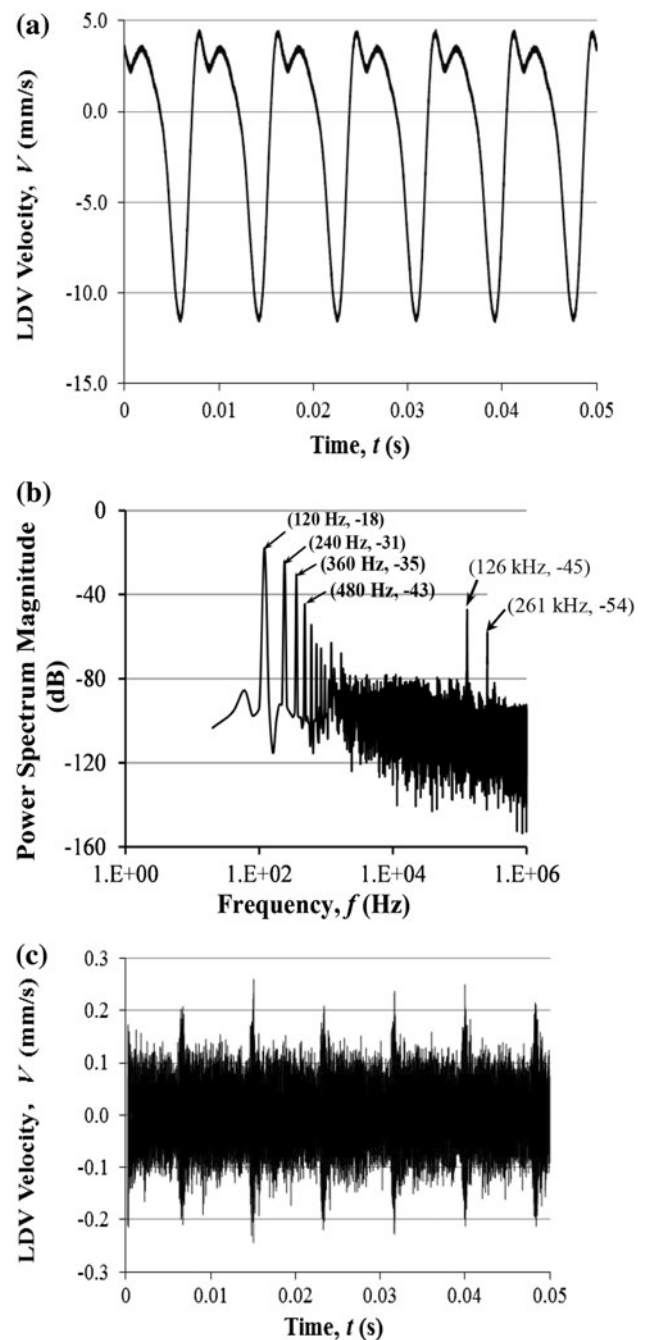


Fig. 3 a original LDV velocity, b FFT analysis of original LDV velocity and c LDV velocity with applying band-pass filter of 20–800 kHz

down power. A further increase in the power input to the heater element above $P_{\text{heat}} = 172$ mW results in a decrease in the amplitude of slider vibrations. This is consistent with the numerical study reported by Zheng and Bogoy (2010). The authors found that the TFC slider becomes unstable when it first makes contact with the disk lubricant, and that with a further increase in the heater element power, slider vibrations decrease.

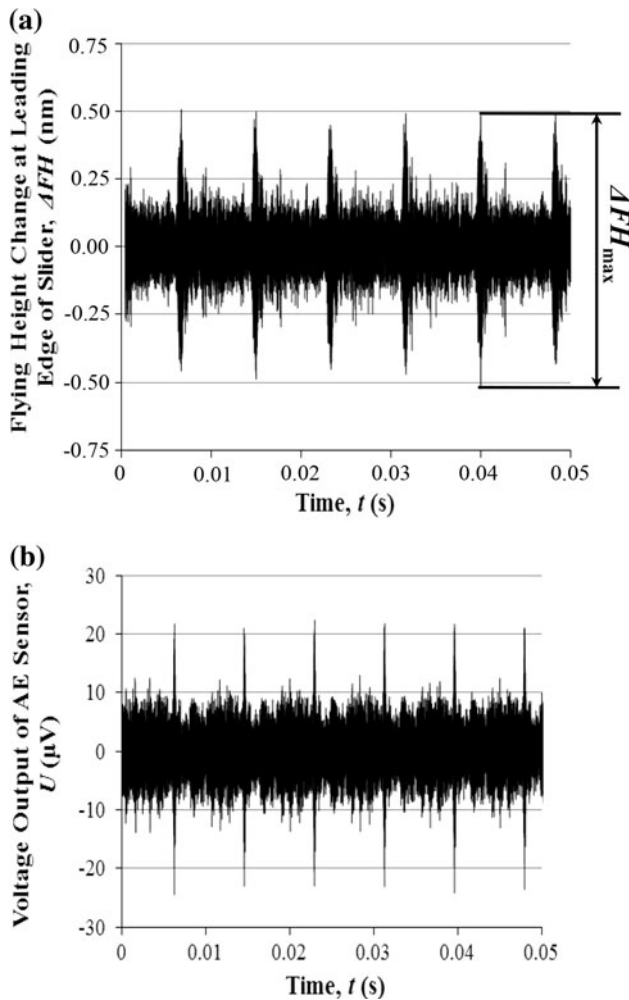


Fig. 4 a flying height change at the leading edge of slider and b voltage output of AE sensor as a function of time

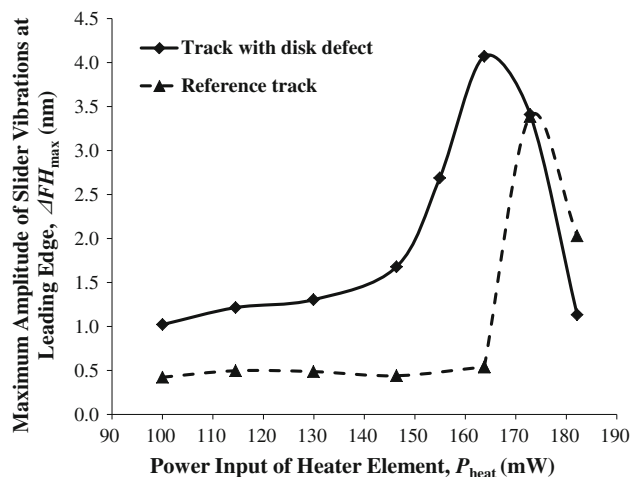


Fig. 5 Maximum amplitude of slider vibrations as a function of power input of heater element in TFC slider

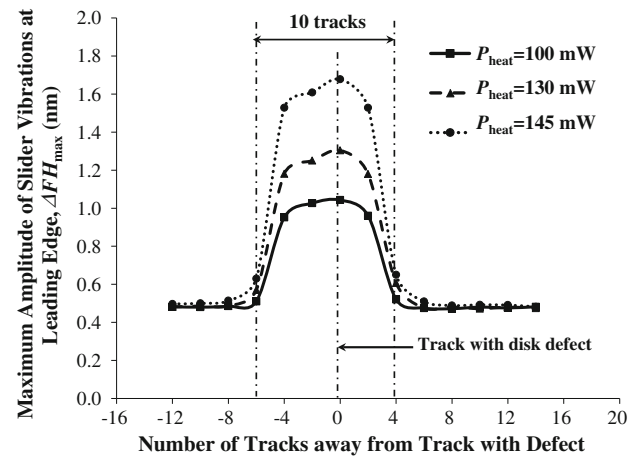


Fig. 6 Maximum amplitude of slider vibrations at leading edge as a function of number of tracks away from track with defect for different values of power input of heater element

For the case when the slider flies over the track with the disk defect, the maximum amplitude of slider vibrations increases monotonically with an increase of power input to the heater element for $P_{\text{heat}} \leq 165$ mW. This is related to an increasing interference between the thermal protrusion of the TFC slider and the disk defect as the power input to the heater element is increased. We also observe that the slider vibrations are larger for the case when the slider flies on the track with the disk defect if $P_{\text{heat}} \leq 175$ mW compared to the case of the reference track. In addition, we observe that the amplitude of slider vibrations for the slider flying on the track with the defect sharply increases at $P_{\text{heat}} \approx 150$ mW. This is lower than for the case of the reference track and indicates that defects on the disk surface can significantly affect the flying characteristics of a slider.

Figure 6 shows the maximum amplitude of the slider vibrations at the leading edge as a function of the number of tracks away from the track with the defect. From Fig. 6 we observe that when the slider flies on the track with the defect, the maximum amplitude of slider vibrations is on the order of 1.7 nm for the heater power input of 145 mW. However, the maximum amplitude of slider vibrations is on the order of 0.5 nm when the slider flies over tracks which are more than six tracks away from the center of the defect. As can be seen from Fig. 6, the disk defect occupies about ten tracks, corresponding to a disk density of 250,000 tracks/inch. This indicates that the width of the defect is about 1 μm assuming the width of one track being approximately 100 nm. The estimated width of the defect is in a good agreement with the physical width of 1.1 μm measured by the AFM. Based on Fig. 6, in order to avoid contacts between the slider and the disk defects, it is recommended to map at least ten tracks around a disk defect, i.e., the slider are not allowed to fly over these tracks.

3 Slider dynamics induced by contacts with artificial asperities

3.1 Preparation of artificial disk asperities

In this study, a nano-indenter (Hysitron TriboScope) was used to create artificial asperities on a disk surface. The shape of the indentations was characterized using a AFM (Digital Instrument 3000). Figure 7 shows an indentation made on a disk with the maximum normal load of 5,000 μN using a blunt tip. The profiles of the dashed lines in Fig. 7a and c are shown in Fig. 7b and d, respectively. From Fig. 7, we observe that the vertical displacement around the indentation can be used to simulate asperities on the disk surface. We denote these simulated asperities as “artificial asperities” in this study. As shown in Fig. 7b and d, a typical artificial asperity has a height h of 11.2 nm and a width w of 1,080 nm. In addition, the shape of the artificial asperities can be varied by using different indentation tips, and by applying different normal loads. Artificial asperities allow the study of slider dynamics.

3.2 Detection of slider contacts with artificial asperities on a spin stand

To obtain the slider dynamics induced by contacts with disk asperities, the location of the artificial asperities has to be identified. In this section, artificial asperities shown in Fig. 7 were detected by an AE sensor mounted on an arm with a head gimbal assembly (HGA) on a spin stand test rig.

Figure 8 shows the experimental setup (MicroPhysics DHT-2) used to detect artificial disk asperities. From the schematic of the experimental setups shown in Fig. 8a, we observe that the disk with the artificial asperity is fixed on the spindle and rotates at an angular velocity of 7,200 rpm. The AE sensor is mounted on the arm which holds the HGA shown in Fig. 8c. The AE signal is amplified by a factor of 1,000 with a commercially available amplifier (Mistras 2/4/6C). Then, the amplified AE signal is captured at 2 MHz sampling rate using the spindle index as a trigger. The power input to the heater element is adjusted by changing the output voltage of a power supplier. The radial location of the HGA is managed by the stage controller of the spin stand system.

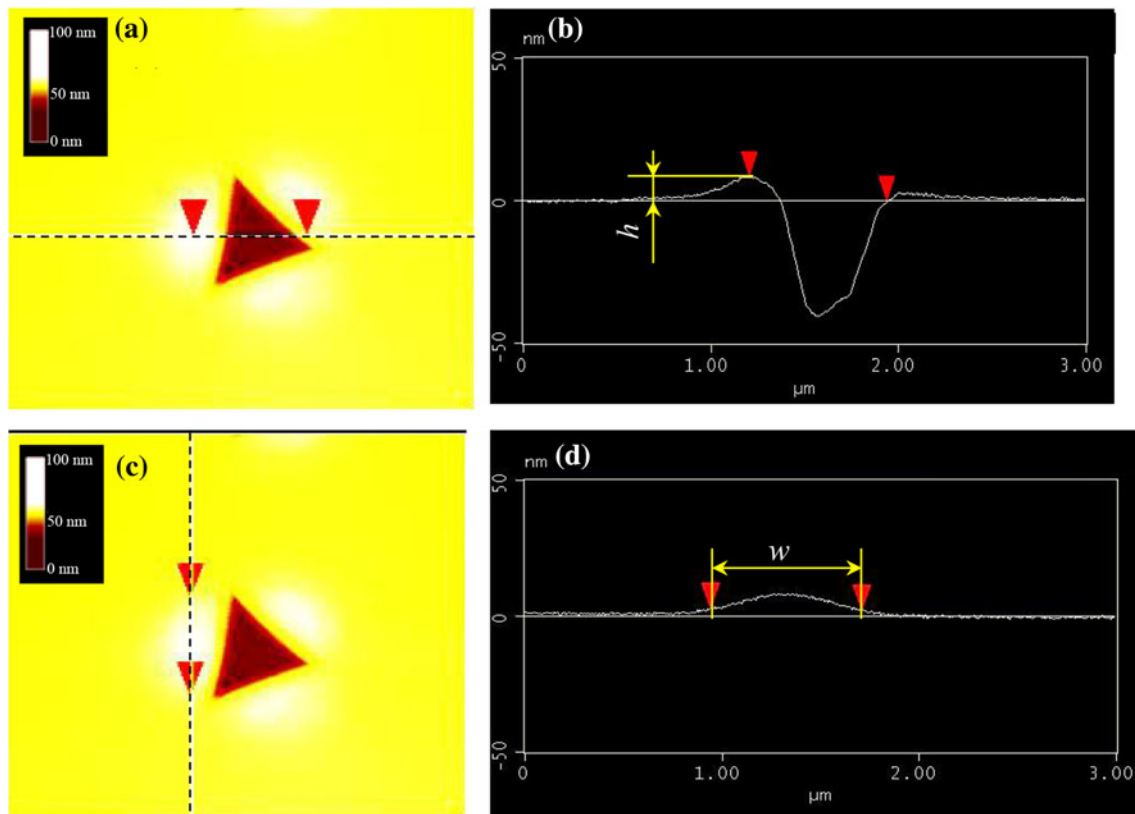


Fig. 7 AFM measurement of artificial asperity

Fig. 8 **a** schematic of experimental setup, **b** spin stand system (Microphysics) and **c** AE sensor on an arm with HGA

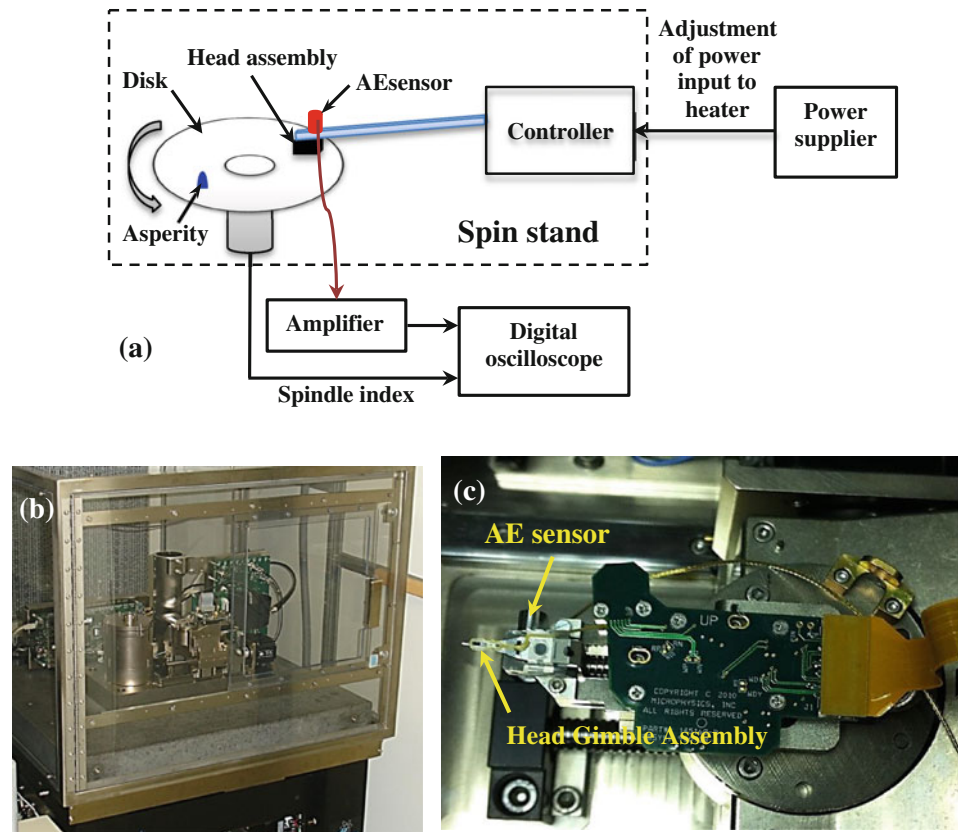


Fig. 9 Voltage output of AE sensor as a function of time for different power inputs to heater element

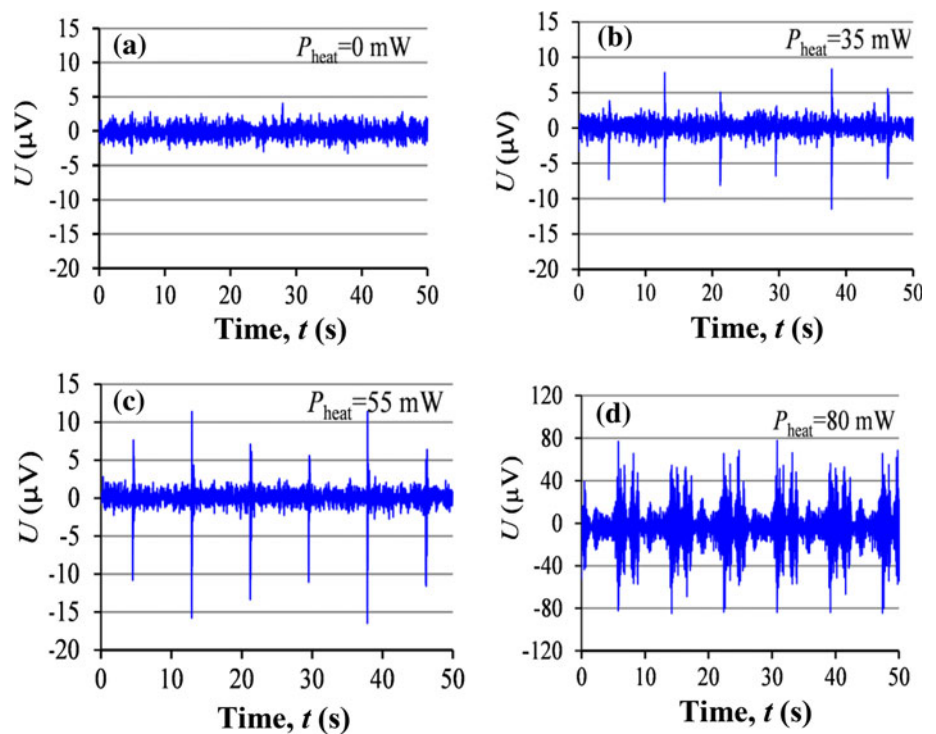


Figure 9 shows the voltage output of the AE sensor as a function of power input of the heater element when the slider is positioned to fly over the artificial asperity

described in Fig. 7. From Fig. 9, we observe that the voltage output from the AE sensor is almost zero when no power is applied to the heater element indicating absence of

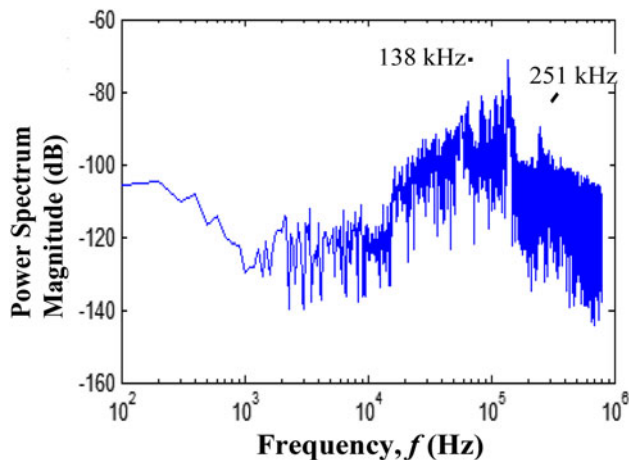


Fig. 10 FFT analysis of AE single shown in Fig. 9b

contacts with the disk. From Fig. 9b and c, periodic vibrations of the slider are detected by the AE sensor for $P_{\text{heat}} = 35 \text{ mW}$ and $P_{\text{heat}} = 55 \text{ mW}$. These periodic vibrations are due to contacts between the TFC slider and the artificial asperity. In addition, we observe that the magnitude of the vibrations of the AE signal increases with increasing power input to the heater element. This is due to the fact that by increasing the power input to the heater element, the effective gap between the slider and the artificial disk asperity decreases resulting in stronger slider to disk interaction. When the power input to the heater element is $P_{\text{heat}} = 80 \text{ mW}$, the AE signal becomes much larger than that shown in Fig. 9b and c. This seems to indicate touchdown.

FFT analysis of the AE signal in Fig. 9c is shown in Fig. 10. From Fig. 10, we observe that the slider vibrations include two distinct frequencies at 138 and 251 kHz corresponding to the first and second pitch slider mode, respectively.

4 Conclusion

The slider dynamics induced by contacts with a disk asperity was studied in a drive level system using thermal flying height control sliders. The slider vibrations were found to be a strong function of the power input to the heater element. For a disk defect with a height of 26 nm

and a width of 1.1 μm , vertical vibrations at the leading edge of the slider were found to be within the maximum amplitude of 4 nm for a power input to the heater element of 165 mW. Based on the drive level data, it is recommended to map out at least 10 tracks around the defect to avoid potential damage of the read/write elements induced by contacts with the defect.

Artificial asperities on a disk surface created by nano-indentation were characterized using AFM. First and second pitch mode slider vibrations due to interactions with artificial disk asperities were observed at frequencies of 138 and 251 kHz, respectively, using AE sensor.

References

- Deoras SK, Talke FE (2003) Slider-lubricant interactions for low flying sliders. *IEEE Trans Magn* 39(5):2471–2473
- Knigge BE, Talke FE (2001) Dynamics of transient events at head/disk interface. *Tribol Int* 34:453–460
- Kurita M, Shiramatsu T, Miyake K et al (2006) Active flying-height control slider using MEMS thermal actuator. *Microsyst Technol* 12(4):369–375
- Li N, Zheng L, Meng Y, Bogy DB (2009) Experimental study of head-disk interface fly ability and durability at sub-1-nm clearance. *IEEE Trans Magn* 45(10):3624–3627
- Nikitin V, Hsiao D, Chen J et al (2007) Challenges for perpendicular write heads at high recording density. *IEEE Trans Magn* 43(2):605–608
- Ovcharenko A, Yang M, Chun K, Talke FE (2010) Simulation of magnetic erasure due to transient slider-disk contacts. *IEEE Trans Magn* 46(3):770–777
- Su L, Hu Y, Lam EL, Li P, Ng RW, Liang D, Zheng O, Liu H, Deng Z, Zhang J (2011) Tribological and dynamic steady of head disk interface at sub-1-nm clearance. *IEEE Trans Magn* 47(1):111–116
- Tanaka H, Yonemura S, Tokisue H (2001) Slider dynamics during continuous contact with textured and smooth disks in ultra low flying height. *IEEE Trans Magn* 37(2):906–911
- Vangipuram S, Bogy DB (2010) Slider dynamics in the lubricant-contact regime. *IEEE Trans Magn* 46(3):764–769
- Wallash A, Zhu H, Chen D (2008) A dynamic scratch test to study read/write head degradation due to head-disk interactions. *IEEE Trans Magn* 44(11):3629–3632
- Zheng J, Bogy DB (2010) Investigation of flying-height stability of thermal fly-height control sliders in lubricant or solid contact with roughness. *Tribol Lett* 38:283–289
- Zheng H, Li H, Talke FE (2009) Numerical simulation of a thermal flying height control slider with dual heater and insulator elements. *IEEE Trans Magn* 45(10):3628–3631